BIOCHEMISTRY
including biophysical chemistry & molecular biology

ARTICLE

pubs.acs.org/biochemistry

Mutational Analysis Reveals a Single Binding Interface between RhoA and Its Effector, PRK1

Catherine L. Hutchinson,[†] Peter N. Lowe,[‡] Stephen H. McLaughlin,[†,§] Helen R. Mott,[†] and Darerca Owen*[,†]

[†]Department of Biochemistry, University of Cambridge, 80 Tennis Court Road, Cambridge CB2 1GA, U.K.

[‡]Biomolecular Interactions Consultancy, 3 Danesbury Park, Hertford SG14 3HX, U.K.

[§]MRC Laboratory of Molecular Biology, Hills Road, Cambridge CB2 0QH, U.K.

Supporting Information

ABSTRACT: Protein kinase C-related kinases (PRKs) are serine/threonine kinases that are members of the protein kinase C superfamily and can be activated by binding to members of the Rho family of small G proteins via a Rho binding motif known as an HR1 domain. The PRKs contain three tandem HR1 domains at their N-termini. The structure of the HR1a domain from PRK1 in complex with RhoA [Maesaki, R., et al. (1999) *Mol. Cell 4*, 793−803] identified two potential contact interfaces between the G protein and the HR1a domain. In this work, we have used an alanine scanning mutagenesis approach to identify whether both contact sites are used when the two proteins interact in solution and also whether HR1b, the second HR1 domain from PRK1, plays a role in binding to RhoA. The mutagenesis identified just one contact site as being relevant for binding of RhoA and HR1a in solution, and the HR1b domain was found not to contribute to RhoA binding. The folded state and thermal stability of the HR1a and HR1b domains were also investigated. HR1b was found to be more thermally stable than HR1a, and it is hypothesized that the differences in the biophysical properties of these two domains govern their interaction with small G proteins.

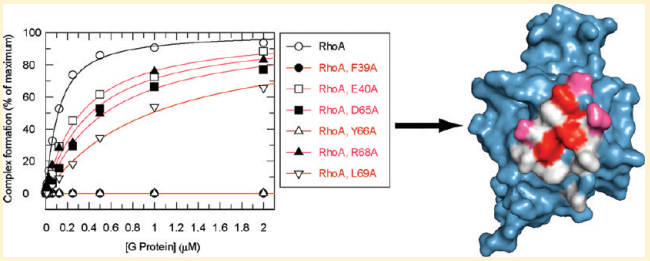

The Ras superfamily small G proteins act as molecular switches that utilize the binding and hydrolysis of GTP to control signal transduction pathways. GTP binding to small G proteins drives a conformational change that permits the G protein to interact with downstream effector proteins, mediating a range of cellular responses. The Rho family of small G proteins controls a wide range of signaling pathways, being best known for their involvement in cell adhesion, growth, and motility through their control of the actin cytoskeleton.[1] Due to their integral role in the regulation of the actin cytoskeleton, Rho family proteins also contribute to pathological processes, including various neuro-developmental disorders such as Fragile X syndrome and Williams syndrome,[2] Alzheimer's disease,[3] and multiple sclerosis;[4] cardiovascular diseases, including hypertension, atherosclerosis, and heart failure;[5] and cell invasion and metastasis in cancer.[6] Rho family proteins are upregulated in many types of human tumors.[6] Understanding how Rho family members contribute to the transforming potential of cells, through deregulation of their signaling pathways at a molecular level, could potentially lead to the development of therapeutics for tackling a wide range of human cancers.

The interaction of Rho proteins with downstream effectors is mediated by recognition motifs known as Rho-binding domains (RBDs). There are at least three classes of RBDs: class I, including those found in the protein kinase C-related kinases (PRKs), rhotekins and rhophilins; class II, including the RBDs in the Rho-associated kinases (ROCKs/ROKs); and class III, including that in Citron.[7] The class I RBDs, also known as HR1 or REM domains, were first identified in the serine/threonine kinase PRK1.[8,9] The PRK proteins PRK1, PRK2, and PKN3 (PRK3) all have the same overall domain structure (Figure 1A). The N-terminal region contains three tandem leucine zipper-like motifs, termed HR1a−c, which are followed by a C2 domain that is related to the calcium-dependent membrane-targeting domain in protein kinase C and a C-terminal kinase domain that is a member of the protein kinase C superfamily.[10]

PRKs have been implicated in the control of a number of important cellular pathways. PRK1 has been shown to mediate control of the cytoskeletal network through phosphorylation of the intermediate filament proteins, neurofilament (subunits L, M, and H), and vimentin.[11,12] PRK1 has also been observed to accumulate in neurofibrillary tangles associated with Alzheimer's disease.[13] PRK1 plays a role in cancer progression: it is overexpressed in prostate cancer, enhancing the transcriptional activity of the androgen receptor,[14] and has been shown to phosphorylate the human papilloma virus E6 oncoprotein, incriminating PRK1 in virally induced cancers.[15]

Received: January 10, 2011
Revised: February 25, 2011
Published: February 25, 2011

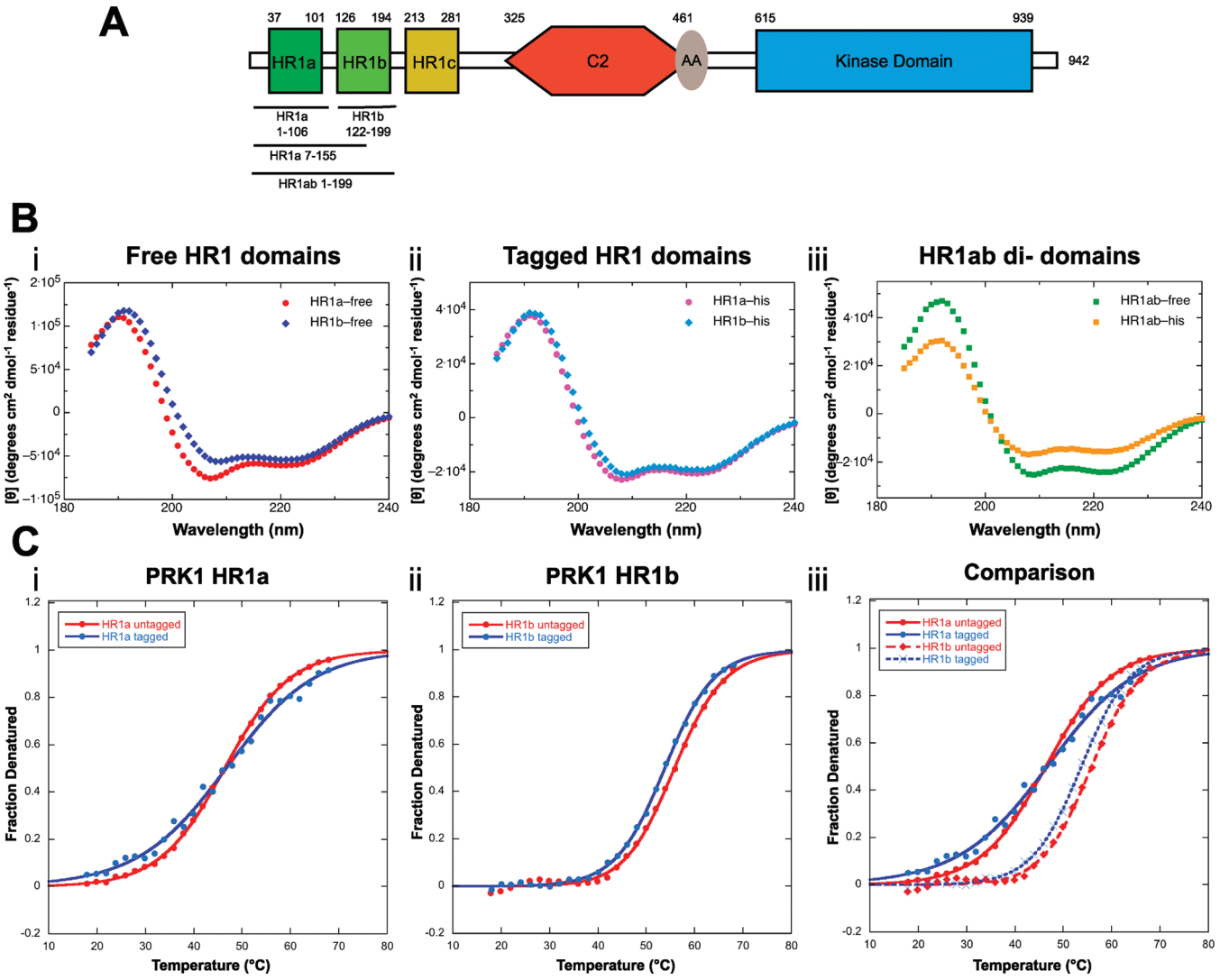

Figure 1. Circular dichroism analysis of the HR1 domains from PRK1. (A) Domain structure of PRK1. PRK1 contains three tandem HR1 domains at the N-terminus, a calcium-binding C2 domain, an arachidonic acid binding domain (AA), and a C-terminal PKC-like serine/threonine kinase domain. The various HR1 constructs used in this work and by Li et al.[36] are marked by black lines. (B) CD spectra of the free and C-terminally His-tagged PRK1 HR1a and HR1b domains. Machine units in millidegrees were converted to mean residue ellipticity in degrees square centimeters per decimole per residue using the Dichroweb[31,32] server and plotted vs wavelength. The characteristic minima at 222 and 208 nm indicate that the domains are helical. There is little difference in the helical content of the free and tagged domains, indicating that the His tag does not interfere with the native fold of the domains. (C) Temperature-dependent melting curves for the free and His-tagged HR1 domains. As described in Methods, the melting temperatures were estimated and the fraction of protein in the denatured state was calculated from the CD signal.

The kinase activity of PRK1 and PRK2 can be activated by their interaction with Rho family small G proteins,[9,16,17] by caspase 3 cleavage during apoptosis,[18] by phosphorylation by the phosphoinositide-dependent protein kinase-1,[19] and by binding fatty acids.[20]

PRK1 binds to Rho family small G proteins through its HR1 motifs; the HR1a domain can bind to both RhoA and Rac1 with high affinity, while the HR1b domain can bind tightly only to Rac1.[21−23] The function of the HR1c domain is presently unknown. The structures of HR1a and HR1b have been determined and show that HR1 domains adopt an antiparallel coiled-coil fold.[22,24] The X-ray structure of RhoA in complex with HR1a identified two potential contact interfaces between the RBD and the small G protein, termed contact I and contact II: only contact II on RhoA encompasses the switch regions.[24] The switch regions of G proteins change conformation upon nucleotide binding and thus confer nucleotide dependence on G protein−effector interactions. A binding interface that does not include the switch regions would imply an effector interaction that is independent of the nucleotide state of the G protein. In contrast, the solution structure of Rac1 in complex with the PRK1 HR1b domain revealed a single interaction interface that did include the switch regions of the small G protein and was similar to the nucleotide-dependent contact II observed in the RhoA−HR1a structure.[25]

The presence of a putative nucleotide-independent binding site for PRK1 on RhoA raises important questions about the regulation of PRK1 activity by RhoA in vivo. It is important to understand the physiological relevance of the sites identified in the X-ray crystal structure not only because of the implications for experimental design in elucidating the mechanisms by which

PRK activity mediates cellular responses but also for the challenges this would present in the design of targeted therapeutics toward RhoA-mediated PRK signaling. Here we present an alanine scanning mutagenesis study to probe the two contact sites on RhoA for the PRK1 HR1a domain, to elucidate the role of the two binding sites in solution, and to generate a toolkit for dissection of the regulation of PRKs and other HR1 domain-containing proteins by Rho family small G proteins.

METHODS

Expression Constructs. *Homo sapiens* RhoA (amino acids 1−186, F25N, Q63L, hereafter termed RhoA) and its mutants were expressed as glutathione *S*-transferase (GST) fusion proteins in the pGEX-2T expression vector (GE Healthcare) by cloning the coding regions into the *Bam*HI and *Eco*RI sites of the vector.

Constructs expressing PRK1 HR1a (residues 1−106), PRK1 HR1b (residues 122−199), and PRK1 HR1ab (residues 1−199) were cloned into the *Bam*HI and *Eco*RI sites of a modified pGEX-4T3 vector[26] that had been further modified to include a PreScission protease cleavage site[27] in place of the enterokinase site, using the QuikChange site-directed mutagenesis kit (Stratagene). This vector produces proteins with a cleavable N-terminal GST tag and a permanent C-terminal His tag. The *H. sapiens* PRK1 template for HR1 domain cloning was a kind gift from P. Parker (Institute of Cancer Research, London, U.K.).

RhoA Mutagenesis. Site-directed mutagenesis of the RhoA expression construct was performed using the QuikChange Multi site-directed mutagenesis kit (Stratagene). The mutations were confirmed by sequence analysis on an automated sequencer (Applied Biosystems Inc.) by the Department of Biochemistry DNA Sequencing Facility, University of Cambridge.

Recombinant Protein Production. GST fusion proteins were expressed in *Escherichia coli* BL21 (Novagen Inc.). Stationary cultures were diluted 1:10 and grown at 37 °C to an A_{600} of 0.8, and protein expression was induced via the addition of 0.1 mM IPTG for 16 h at 20 °C. Proteins were then purified using glutathione−agarose beads (Sigma-Aldrich) following the manufacturer's instructions. GST-HR1-His domains were eluted from the glutathione beads and cleaved from the GST tag using PreScission protease (GE Healthcare) and the His-tagged HR1 domains purified using Ni-IDA resin (Novagen). The RhoA mutants were cleaved from their GST tag with thrombin (Novagen), while still attached to the beads. All of the proteins were further purified by gel filtration on a Superdex 75 16/60 HiLoad gel filtration column (GE Healthcare), prior to use in assays. Protein concentrations for the RhoA proteins were evaluated from measurement of their A_{280} using their amino acid composition and the extinction coefficients of tyrosine, phenylalanine, tryptophan, and the guanine nucleotide.[28] The concentrations for the HR1 domains were determined using amino acid analysis in the Protein and Nucleic Acid Chemistry facility at the Department of Biochemistry, University of Cambridge.

Nucleotide Exchange. RhoA and its mutants were labeled with [^{3}H]GTP for use in binding assays as described previously.[29]

Scintillation Proximity Assays (SPA). Affinities of RhoA and its mutants for the HR1-His domains were measured using SPA. The His-tagged effector proteins, at constant concentrations of 60 nM, were immobilized on Protein A SPA fluoromicrospheres via an anti-His antibody (Sigma-Aldrich). The equilibrium binding constants (K_d) of the effector−G protein interaction were determined by monitoring the SPA signal in the presence of varying [^{3}H]GTP·RhoA concentrations as described previously.[30] Binding of RhoA to the effector protein brings the radiolabeled nucleotide sufficiently close to the scintillant to yield a signal. For each RhoA variant, an experiment was performed in the absence of effector, which resulted in a linear increase in background SPA counts. This data set was then subtracted from the data points obtained in the presence of effector and plotted as a function of increasing G protein concentration. For each affinity determination, data points were obtained for at least 10 different G protein concentrations. Binding curves were fitted using a direct binding isotherm[30] to yield K_d values and their standard errors for the G protein−effector interactions.

Circular Dichroism. Secondary structure and thermal stability were assessed by circular dichroism. Free HR1 domains and HR1-His domains were buffer exchanged into 10 mM potassium phosphate (pH 7.5) and 100 mM sodium fluoride. Spectra were recorded at a protein concentration of 0.01 mg/mL in a 0.1 mm path length quartz cuvette. Three wavelength scans were recorded for each protein between 250 and 180 nm. The spectra of the free HR1a domains were recorded on an Applied Photophysics Chirascan attached to a TC125 temperature controller from Quantum Northwest, and the spectra of the HR1-His domains were recorded on an AVIV 410 machine. The spectra of both the free and His-tagged HR1ab didomain were recorded on the AVIV 410 machine. Secondary structure prediction was performed on DICHROWEB[31,32] using CDSSTR[33,34] and reference set 3. Thermal stability was determined by following the temperature dependence of the ellipticity of the HR1 domains at 222 nm between 18 and 70 °C in 2 °C increments with a 30 s equilibration time. The fraction of denatured protein can be calculated using the following equation, where θ_T is the signal at a given temperature, θ_N is the signal of native state, and θ_D is the signal of the fully denatured state.

$$\mathrm{frac_D} = \frac{\theta_T - \theta_N}{\theta_D - \theta_N} \quad (1)$$

Because both θ_N and θ_D depend on temperature, the absorbance data were transformed using the following equation:

$$\mathrm{frac_D} = \frac{\theta_T - (\theta_N^0 + \alpha_N T)}{\theta_D^0 + \beta_D T - (\theta_N^0 + \alpha_N T)} \quad (2)$$

The melting temperature (T_m) was then calculated from the stability using the relationship

$$\mathrm{frac_D} = \left[\exp\left(\frac{-1}{RT}\left\{\Delta H_{T_m}\left(1 - \frac{T}{T_m}\right) + \Delta C_p\left[(T - T_m) - T\ln\left(\frac{T}{T_m}\right)\right]\right\}\right)\right] \Big/ \left[1 + \exp\left(\frac{-1}{RT}\left\{\Delta H_{T_m}\left(1 - \frac{T}{T_m}\right) + \Delta C_p\left[(T - T_m) - T\ln\left(\frac{T}{T_m}\right)\right]\right\}\right)\right] \quad (3)$$

where ΔH_{T_m} is the enthalpy of folding and ΔC_p is the change in heat capacity upon folding (for derivation, see the Supporting Information).

RESULTS

Design of the HR1 Domain Fusion Protein Constructs and Optimization of Experimental Conditions. Several observations had led us to believe that the fusion tags used to display

Table 1. CD Analysis of the HR1 Domains

	helical content[a] (% residues)					
	untagged		His-tagged		melting temperature (°C)	
construct	actual	expected	actual	expected	untagged	His-tagged
HR1a	78	78	77	63	46.3 ± 0.1	46.6 ± 0.3
HR1b	69	70	55	54	55.8 ± 0.1	53.8 ± 0.1
HR1ab	79	70	53	63	not available	not available

[a] Helicity percentages reported are the total for both α-helix and 3_{10}-helix combined.

coiled-coil domains were influencing their binding to small G proteins. Previous work with the Ral-binding domain of RLIP76 demonstrated that an N-terminal GST fusion tag caused a significant decrease in the affinity for RalA and RalB.[35] Insertion of a flexible linker between the GST and the coiled-coil domain did not alleviate the problem. For the RLIP76 domain, a C-terminal His tag allowed high-affinity binding to RalA and RalB. Previous work using N-terminal GST fusions of the HR1 domains from PRK1 had yielded reproducible, high affinities,[22,25] but further investigations showed that in fact these interactions were strongly dependent on temperature (data not shown), leading us to conclude that both the fusion tag and the experimental temperature might be influencing the affinity of these coiled-coil domains for small G proteins. In our experience, the HR1 domains of PRK1 are most stable in protein binding assays with the addition of a C-terminal His tag (as used in this study) and with an experimental temperature no greater than 18 °C.

Helicity and Thermal Stability of HR1 Domains of PRK1. Our observation of temperature dependence in binding experiments prompted us to investigate the thermal stability of these domains. Recent work by Li et al.[36] showed that the PRK1 construct, comprising residues 7−155, used to determine the structure of the RhoA−PRK1 HR1a complex[24] was only 18% helical in solution at 4 °C. HR1a residues 7−155 are predicted to be at least 43% helical, even if the assumption is made that residues 122−155 are unstructured. Residues 122−155 lie within the HR1b domain, but as the domain is truncated, we assume that the HR1b helices will be destabilized. If the residues from HR1b were also helical, the expected percentage of helical content would be even higher. Structural analysis of the minimal HR1a domain (residues 1−106) used in our binding studies[22,25] has never been performed. Since residues 7−155 have been shown to be only partially folded[36] and as we had identified a temperature dependence of the affinities of HR1 domains for RhoA, the folded state and thermal stability of HR1a, HR1b, and HR1ab used in this study were analyzed using circular dichroism (Figure 1B). These data were then compared to those of the HR1-His domains that were used in subsequent binding experiments to ensure that addition of the tag did not affect the folded state of the domains (Figure 1B and Table 1). Both the untagged and tagged single domains show at least the expected secondary structure content at 18 °C and are helical. On the basis of the published structures of the two domains, it would be expected that HR1a would be 78% helical and HR1b 70% helical. Assuming that the linker between the domains is unstructured (as indeed is predicted by GLOBplot[37] and PredictProtein[38]), the didomain, HR1ab, should therefore be approximately 70% helical. Interestingly, the analysis of the CD data for the free HR1ab domain shows a slightly higher percentage helicity than expected while the His-tagged HR1ab domain has a slightly lower helical content.

Analysis of the thermal stability of the HR1 domains revealed that the addition of a C-terminal His tag did not adversely affect the stability of the domains. However, the HR1a domain had a melting temperature ∼10 °C lower than that of the HR1b domain (Figure 1C and Table 1). At 26 °C, these CD studies showed that HR1b was not detectably unfolding, whereas HR1a was already 5% unfolded. In contrast, at 18 °C, both HR1a and HR1b were fully folded. These data support the observation that both HR1 domains bind reproducibly and with high affinity to Rho family G proteins at a temperature no greater than 18 °C.

Design of the RhoA Mutants. The structure of the RhoA−PRK1 HR1a complex[24] was used to identify residues on RhoA that contact the HR1a domain. The residues that were selected were those located in either the contact I or contact II interface whose side chain atoms were within 4 Å of RhoA and therefore likely to contribute to binding. In total, 20 residues were identified, 10 in the contact I interface and 10 in the contact II interface: Lys27, Asp28, Gln29, Asp45, Glu47, Gln52, Glu54, Lys164, Arg168, and Gln169 in contact I and Val38, Phe39, Gln40, Asn41, Asp65, Tyr66, Arg68, Leu69, Leu72, and Asp76 in contact II. These residues are depicted on a surface representation of RhoA in Figure 2A,B.

Alanine scanning mutagenesis was used to identify the contribution that these amino acids made to the energetics of the binding interface. Alanine substitution at a given residue removes all side chain atoms except the β-carbon, but unlike glycine, it does not introduce conformational flexibility into the protein backbone. This allows affinity data gathered from alanine mutants to be used to calculate the specific contribution of a given residue to the energy of binding. Those residues that contribute significantly to the binding energy of an interaction are commonly termed hot spots.[39]

HR1a Binding Occurs through the Contact II Interface. The affinities of the 20 RhoA mutants for the HR1a domain from PRK1 were determined using scintillation proximity assays (SPA). The apparent K_d values for the mutants were compared to that for RhoA to determine mutations that reduced the affinity of RhoA for PRK1 HR1a. The apparent K_d values for all 20 mutants are listed in Table 2, and binding data for selected mutants are shown in Figure 2C,D. The residues in which mutation to alanine significantly reduced the affinity of RhoA for the PRK1 HR1a domain were $Phe39^{RhoA}$, $Glu40^{RhoA}$, $Asp65^{RhoA}$, $Tyr66^{RhoA}$, $Arg68^{RhoA}$, and $Leu69^{RhoA}$ (Figure 2D). All of these residues lie in the contact II interface identified in the X-ray crystal structure, and no residues in contact I were found that significantly reduced the affinity of RhoA for PRK1 (Figure 2C). This suggests that the solution interaction interface between RhoA and the HR1a domain from PRK1 is contact II.

The HR1b Domain Does Not Contribute to the Binding of PRK1 with RhoA. Since the crystal structure identified two binding interfaces for PRK1 HR1a on RhoA, we had previously hypothesized that the contact I interface could be used in solution by the HR1b domain to reinforce the RhoA−PRK1 interaction once HR1a engages the contact II interface.[25] To test this hypothesis, we investigated the suite of RhoA mutants for their ability to bind to the PRK1 HR1ab didomain. The apparent K_d values were again compared with those of RhoA to identify those mutants that reduced the affinity of RhoA for the didomain.

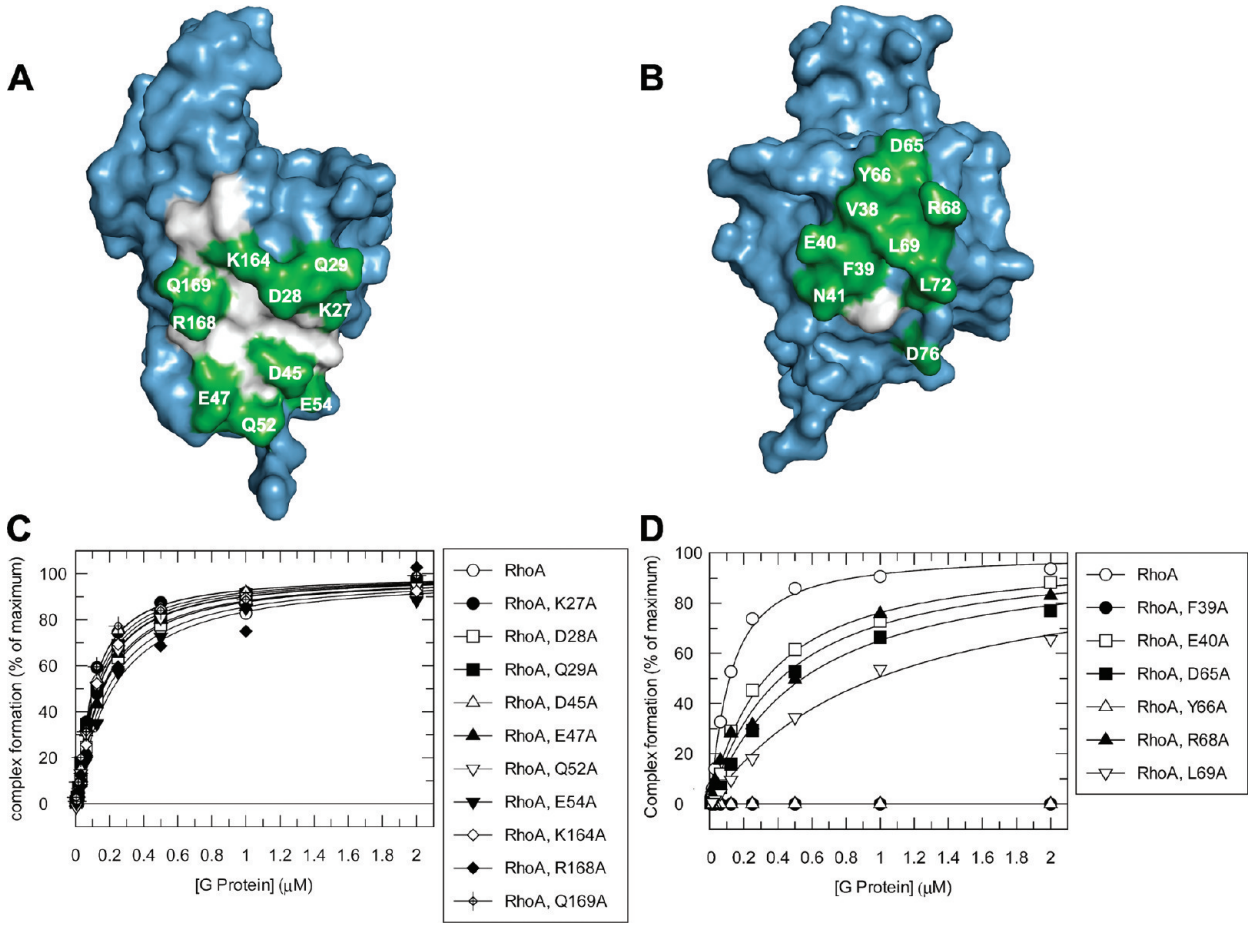

Figure 2. Surface representation of RhoA showing residues in contact sites I and II for the PRK1 HR1a domain and the measurement of the affinity of RhoA and selected mutants for HR1a. (A and B) Surface representations of the two contact interfaces on RhoA for PRK1 HR1a. The RhoA protein is colored blue with those residues identified from the crystal structure as part of the PRK1 HR1a interface highlighted in white.[24] Residues with side chains within 4 Å of the HR1a domain were chosen for mutation and are highlighted in green: (A) contact I interface and (B) contact II interface. (C and D) The indicated concentration of [^{3}H]GTP-labeled G protein was incubated with His-tagged effector protein in SPA. A constant concentration of 60 nM HR1a-His was used in these experiments. The SPA signal was corrected by subtraction of a background signal from parallel measurements in which the effector fusion protein was omitted. The effect of the concentration of G protein on this corrected SPA signal was fitted to a binding isotherm to give an apparent K_d value and the signal at saturating G protein concentrations. The data and curve fits are displayed as a percentage of this maximal signal: (C) binding isotherms of all the contact I mutants and (D) binding isotherms of contact II mutants with a reduced affinity for PRK1 HR1a-His.

The results are listed in Table 2. In these experiments, no major differences were observed in the relative affinities of RhoA for the HR1a domain alone as compared with the affinity of RhoA for the HR1ab didomain; those mutants that were found to reduce the affinity of RhoA for the HR1a domain alone also reduced the affinity of RhoA for the didomain by a similar amount. These data indicate that, in the HR1ab didomain, only the HR1a domain is contacting RhoA and that the interaction occurs through the contact II interface.

DISCUSSION

The aim of this work was to establish the role of the two binding interfaces on RhoA for the PRK1 HR1a domain identified by structural studies.[24] Mutations were designed across the two interfaces both to indicate which of the two contact sites in the crystal structure were relevant in solution and to define energetic hot spots underpinning the interaction of RhoA and PRK1. The data presented here identified only residues in contact II as being energetically involved in the binding interaction.

In an initial analysis of the structure of the RhoA−PRK1 HR1a complex, contact I was identified as the most likely binding interface between RhoA and PRK1: it buried a surface area of 2080 Å^2 and was made up of a network of hydrogen bonds and salt bridges. In contrast, contact II buried only 1640 Å^2 and was a largely hydrophobic interface.[24] The data presented here show that only mutants in contact II reduce the affinity of RhoA for PRK1 HR1a; therefore, these observations together identify contact II as the relevant solution binding site for PRK1 HR1a on RhoA. Binding at contact II is more typical of an effector interface on a G protein because of the involvement of the switch regions. Conversely, PRK1 binding to RhoA at the contact I interface would not have involved the switch regions of RhoA. This would have implied that the binding of the two proteins would not be sensitive to the nucleotide state of the small G protein, whereas previous work has indicated that PRK1 does indeed show a preference for RhoA·GTP over RhoA·GDP.[21,23]

By combining the data generated in this study with the X-ray crystal structure of the RhoA−PRK1 HR1a complex, we are now able to build a more detailed picture of the true solution interface

Table 2. Apparent Dissociation Constants for the RhoA Mutants Binding to PRK1 HR1 Domains

	apparent K_d (nM)		ΔG (kcal mol^{-1})		$\Delta\Delta G$ (kcal mol^{-1})		x-fold change in affinity	
	HR1a	HR1ab	HR1a	HR1ab	HR1a	HR1ab	HR1a	HR1ab
RhoA	97 ± 12	156 ± 21	−9.56	−9.28				
contact I								
K27A	72 ± 20	33 ± 8	−9.73	−10.19	0.17	0.91	1.4	5.0
D28A	132 ± 14	141 ± 21	−9.37	−9.34	−0.19	0.06	−1.4	1.1
Q29A	93 ± 6	156 ± 25	−9.58	−9.28	0.02	–	none	none
D45A	84 ± 10	238 ± 36	−9.64	−9.03	0.08	−0.25	1.1	−1.5
E47A	133 ± 16	122 ± 22	−9.37	−9.42	−0.19	0.14	−1.4	1.3
Q52A	105 ± 12	131 ± 28	−9.51	−9.38	−0.05	0.10	−1.1	1.3
E54A	187 ± 22	44 ± 4	−9.17	−10.02	−0.39	0.74	−1.9	3.3
K164A	102 ± 14	122 ± 27	−9.53	−9.42	−0.03	0.14	−1.1	1.3
R168A	160 ± 43	232 ± 60	−9.26	−9.04	−0.30	−0.24	−1.6	−1.5
Q169A	73 ± 10	142 ± 16	−9.72	−9.33	0.16	0.05	1.3	1.1
contact II								
V38A	19 ± 4	82 ± 10	−10.52	−9.66	0.96	0.38	5.0	2.0
F39A	≥1000	≥1000	≥−8.18	≥−8.18	≥−1.38	≥−1.10	−10.3	−6.4
E40A	298 ± 36	684 ± 120	−8.89	−8.4	−0.67	−0.88	−3.1	−4.4
N41A	22 ± 4	56 ± 7	−10.43	−9.88	0.87	0.60	5.0	2.5
D65A	515 ± 77	≥1000	−8.57	≥−8.18	−0.99	≥−1.10	−5.3	−6.4
Y66A	≥1000	≥1000	≥−8.18	≥−8.18	≥−1.38	≥−1.10	−10.3	−6.4
R68A	390 ± 78	529 ± 47	−8.73	−8.55	−0.83	−0.73	−4.0	−3.4
L69A	947 ± 122	≥1000	−8.21	≥−8.18	−1.35	≥−1.10	−9.8	−6.4
L72A	17 ± 7	53 ± 4	−10.59	−9.91	1.03	0.63	5.0	3.3
D76A	20 ± 5	76 ± 7	−10.49	−9.7	0.93	0.42	5.0	2.0

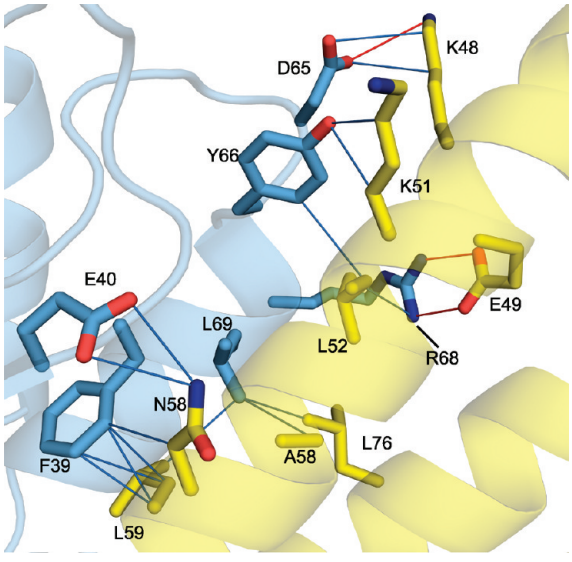

Figure 3. Interaction interface between RhoA and PRK1 HR1a. The residues involved in the interaction between RhoA and PRK1 HR1a are shown as sticks. RhoA residues are colored blue and HR1a residues yellow. Nitrogen atoms are colored dark blue and oxygen atoms red. Side chain atoms that are within 4 Å of each other are linked by blue lines. Hydrogen bonds between side chains are represented as red lines.

between RhoA and PRK1 and create an energy landscape for the interaction. Figure 3 shows contact II in the crystal structure, highlighting residues on RhoA that are now known to be thermodynamically involved in complex formation. Also highlighted are the relevant residues in HR1a that are the likely contacts for these RhoA residues. The F39A mutation reduced the affinity of RhoA for HR1a by >10-fold (Table 2 and Figure 2D). The ring of Phe39^{RhoA} contacts the side chain of Leu59^{PRK1} in the structure of the RhoA−PRK1 HR1a complex[24] (Figure 3), and mutating Leu59^{PRK1} to Lys abrogated binding to RhoA,[36] highlighting this contact as an important mediator of the interaction. Furthermore, as Phe39 is in the center of the interface, the removal of the aromatic ring when Ala replaces Phe is likely to lead to rearrangements of several side chains. The E40A mutation, which is also in switch I, decreases the affinity of RhoA for HR1a by ~3-fold (Table 2 and Figure 2D). The side chain of Glu40^{RhoA} forms hydrogen bonds with Asn58^{PRK1}, but these presumably do not contribute a large amount to the energy of the interaction, because their loss reduces the affinity only 3-fold. Glu40^{RhoA} is on the edge of the interface, so its replacement with Ala is unlikely to affect other interactions. Interactions with residues in switch II are also important for affinity. Asp65^{RhoA} forms a salt bridge with Lys48^{PRK1}, and loss of this interaction leads to a 5-fold reduction in affinity (Table 2 and Figure 2D). On the other hand, mutation of Tyr66^{RhoA} decreases the affinity for HR1a by >10-fold (Table 2 and Figure 2D) because of the loss of contacts between the tyrosine ring and Lys51^{PRK1} and Leu52^{PRK1}. Again, the loss of the aromatic ring when Ala replaces the Tyr is likely to cause structural rearrangements in this region as well. Arg68^{RhoA} forms a salt bridge with Glu49^{PRK1}, and its loss decreases the affinity of RhoA for HR1a by 4-fold. The L69A mutation shows a decreased affinity for PRK1 HR1a of ~10-fold (Table 2 and Figure 2D). Like F39^{RhoA},

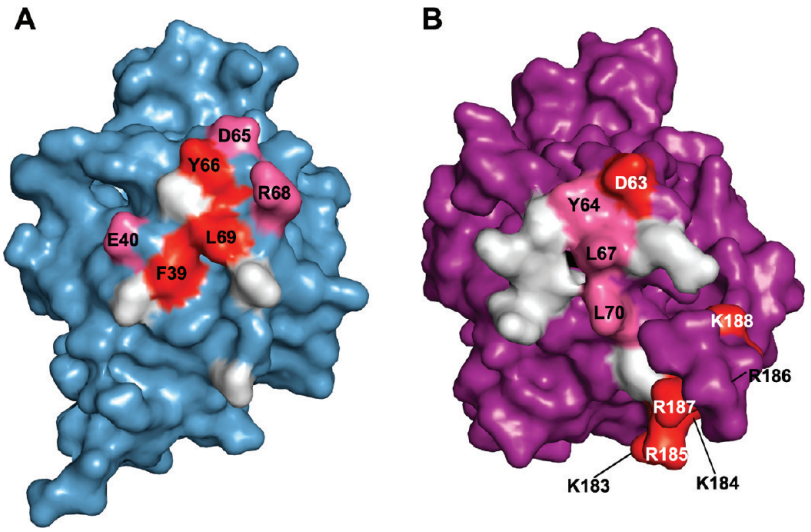

Figure 4. Comparison of the energetic hot spots for HR1 domains binding to Rac1 and RhoA. (A) The surface representation of RhoA is colored blue. The residues involved in interaction with the HR1a domain are colored as follows: pink for those residues that reduce the affinity of the HR1 domain for the G protein ~3−6-fold, red for those residues that reduce the affinity of the HR1 domain for the G protein ≥8-fold, and white for all others. (B) The surface representation of Rac1 is colored magenta. The residues involved in interaction with the HR1b domain are colored as in panel A. Identification of the hot spots for the Rac1−HR1b interaction was based on our previous mutagenesis data.[22].

Leu69^{RhoA} also contacts Leu59^{PRK1}, which has been demonstrated to be critical for the RhoA−HR1a interaction. Both F39^{RhoA} and Leu69^{RhoA} contribute significantly to the energetics of the binding interaction. Phe39^{RhoA} contributes at least 14% of the total binding energy (Table 2). Leu69^{RhoA} contributes 13.7% of the total binding energy (Table 2), and therefore, it is not surprising that Leu59^{PRK1} is a key mediator of RhoA binding.

This study also pinpoints residues in contact II that when mutated to alanine actually increase the affinity of RhoA for HR1a and HR1ab. Some of these changes can be rationalized by analysis of the structure.[24] The V38A mutation increases the affinity for HR1a (5-fold) and that for HR1ab (2-fold) (Table 2). Val38^{RhoA} contacts Leu52^{PRK1} and Lys51^{PRK1}, and presumably, its replacement with Ala allows closer packing, possibly allowing a tighter interaction between Tyr66^{RhoA} and Lys51^{PRK1}. The N41A mutation increases the affinities for HR1a and HR1ab by 5- and 2.5-fold, respectively (Table 2). The Asn41^{RhoA} side chain does not make any polar contacts with PRK1, and its replacement with Ala would allow hydrophobic interactions with Ala62^{PRK1} and therefore closer packing in this part of the interface. The D76A mutation increases the affinity for HR1a 5-fold and that for HR1ab 2-fold (Table 2). Asp76^{RhoA} actually makes a salt bridge with Arg68^{PRK1}. However, Arg68^{PRK1} is in the loop between the two helices of HR1a, which is likely to be relatively flexible because it has an increased temperature factor in the crystal structure.[24] The entropic gain when Arg68^{PRK1} is released by the loss of the interaction with Asp76^{RhoA} possibly offsets the loss of the favorable enthalpic salt bridge. In addition, the Ala76^{RhoA} mutant could now make hydrophobic contacts with Leu66^{PRK1}, which would also be entropically favored as Leu66^{PRK1b} is solvent-exposed in the RhoA−PRK1 HR1a complex.

Figure 4A shows the energetic hot spots on RhoA for the HR1a interface. The six residues identified as mediating the PRK1−RhoA interaction together could contribute 65% of the binding energy of the interaction (calculated from the data in Table 2 by summing the individual contributions of residues). Phe39^{RhoA}, Tyr66^{RhoA}, and L69^{RhoA} make the greatest contribution to affinity.

Li et al.[36] recently used a protein grafting approach to study the interaction between RhoA and the HR1a domain from PRK1. A stable scaffold was made using the antiparallel coiled-coil (ACC) domain from *E. coli* seryl tRNA synthetase (SRS). This SRS scaffold was then mutated to contain those residues from PRK1 HR1a that contacted RhoA in the crystal structure.[24,36] Using this approach, which investigates the role of PRK1 HR1a residues in binding to RhoA and as such is complementary to the work presented here, Li et al. drew similar conclusions, in that contact II is the relevant solution binding site.

Li et al. also used CD to investigate the folded state of the HR1a domain from PRK1 (using amino acids 7−155, the residues crystallized for the structure of the PRK1 HR1a−RhoA complex) compared to the grafted SRS−ACC scaffold. These data indicated that the scaffold-based hybrid protein contained more helix in solution than the PRK1 construct, which was significantly less helical than expected. This was a surprising result as the data presented here demonstrate that the HR1a domain of residues 1−106 contains the expected proportion of helix at 18 °C (Figure 1 and Table 1). The construct of residues 7−155 of PRK1 contains all of HR1a and half of HR1b. The different helical content of the two constructs suggests that the presence of the extra residues (107−155) influences the overall structure of the HR1a domain. Conversely, the data we present for the HR1ab didomain show slightly more helix than would be predicted on the basis of the secondary structures of the isolated HR1a and HR1b domains combined. Addition of the C-terminal His tag made the HR1ab construct slightly less helical than expected. This was not observed with the isolated HR1 domains. Despite this apparent reduction in helicity, the HR1ab domain was still able to bind tightly to RhoA. Because no structural data for the didomain are available, it is not possible to determine how the didomain differs in structure from HR1a or HR1b in isolation. It is, however, evident that the didomain is not simply a sum of its two component parts.

The SRS−ACC scaffold with PRK1 contact I residues grafted onto the surface was unable to bind to RhoA, while the scaffold

with contact II residues grafted onto it could bind with a K_d of 1.7 μM. However, the HR1a domain itself in the same study (residues 7−155) bound significantly more tightly (K_d = 530 nM). Both of these affinities are weaker than that determined for the C-terminally His-tagged HR1a domain of residues 1−106 used in this study (97 nM). This could reflect the different assay conditions used in the two studies (SPR vs SPA) or may be indicative of true differences in affinities of the three different constructs. Differences in affinity for RhoA between the PRK1 domain of residues 7−155 and the SRS−ACC contact II scaffold (both measured by SPR), however, may indicate that apart from the surface contact residues there are more subtle factors that affect the affinity of the HR1 domain for RhoA. Li et al. demonstrate that PRK1 residues 7−155 manifest only 18% helicity, suggesting that only a proportion of the molecules in solution adopt the coiled-coil structure; the contact II scaffold on the other hand displays 83% helicity, suggesting that the majority of the population is folded. Data presented in this work show that the melting temperature of the HR1a domain (residues 1−106) is 46 °C, 10 °C lower than the values of 56 °C for the SRS−ACC contact II scaffold. Furthermore, both PRK1 HR1a constructs (residues 7−155 and 1−106) have a higher affinity for RhoA than does the contact II scaffold, implying that the innate flexibility of the native PRK1 HR1a domain is required for high-affinity RhoA binding. Employing a stable-scaffold approach naturally reduces this flexibility. We have observed in previous studies with small G protein−effector interactions that the molecular topography of the G protein binding surface can be crucial for effector binding: residues behind the contact surface had significant effects on the affinity of the interaction between Cdc42 and ACK.[40] This implies that the flexibility of regions outside the direct interaction surface could indeed have an effect on binding other molecules. Interestingly, the melting temperatures of the HR1b domain from PRK1 and the SRS−ACC contact II scaffold exhibit similar thermal stability (T_m of 56 °C for each). It is possible that part of the reason that the more stable HR1b domain cannot bind RhoA is that it lacks some of the conformational flexibility of the HR1a domain.

We hypothesized previously that, while not able to bind to RhoA on its own, the HR1b domain might strengthen the RhoA−PRK1 interaction by occupying the contact I site once HR1a was bound at contact II. Binding of the HR1ab double domain to RhoA was indistinguishable from that of the HR1a domain alone. This implies that the role of the two HR1 domains in PRK1 is to bind to RhoA and Rac1, respectively, and that the two HR1 domains do not bind to a single RhoA molecule simultaneously.

The residues in the contact II interface on RhoA are either identical or highly conserved with those at the interface between HR1b and Rac1, but a comparison of the energetic hot spots on these two surfaces as determined by mutational analysis reveals marked differences in thermodynamics (Figure 4A,B). The Rac−HR1b interaction shows an unusual contact site on Rac1 as it involves the C-terminal polybasic region of the small G protein.[25] In fact, at least 16% of the energy for the binding of HR1b to Rac1 is contributed by these C-terminal residues (183−188), which lie at the periphery of the binding interface (Figure 4B).[25] For HR1a binding to RhoA, the hot spots are concentrated in the center of the binding interface. The degree of contribution of specific residues to the energetics of the binding interaction is also quite different for the two proteins. $Tyr64^{Rac1}$ and $Leu67^{Rac1}$ make only small contributions (3 and 11%, respectively) to the binding energy for HR1b, and $Phe37^{Rac1}$ does not contribute at all.[22] This is in contrast to the RhoA−HR1a interaction where both $Phe39^{RhoA}$ (Phe37 in Rac1) and $Tyr66^{RhoA}$ (Tyr64 in Rac1) completely abrogate binding (Table 2 and Figure 2) and $Leu69^{RhoA}$ (Leu67 in Rac1) reduces the level of binding to HR1a 10-fold (Table 2 and Figure 2). Interestingly, despite all of the residues that have been identified as being important for mediating RhoA−HR1a binding being conserved at the Rac1−HR1b surface, Rac1 still requires its C-terminal polybasic region to bind to HR1a and HR1b. The differences in energy contributions by the conserved residues in the two complexes and their diminished contributions in the Rac1−HR1b complex underpin the requirement for other areas of the protein to contribute to the Rac1−HR1b binding interface. Thus, the differing contributions of interface residues acting in combination with the contrasting use of the polybasic region are what makes HR1b specific for Rac1 and yet still allows HR1a to bind both RhoA and Rac1.

The question of the mode of binding that PRK1 uses to interact with these two G proteins remains. The data we present here rule out the possibility that RhoA simultaneously binds HR1a and HR1b.[25] We also proposed an alternative model in which RhoA and Rac1 could bind simultaneously to PRK1. The linker between the two HR1 domains is sufficient to allow binding of the two G proteins, and this model should still be viable using the contact II interface on RhoA. It may also be that the two HR1 domains act independently and serve to direct the functions of PRK1 in response to various stimuli, as subcellular localization would affect whether RhoA and Rac1 could bind to PRK1 simultaneously in vivo. HR1a contains a putative pseudosubstrate site,[41] and because this domain binds to both RhoA and Rac1, both should be capable of activating the kinase. In fact, this has been shown to be the case for the *Drosophila melanogaster* PRK1 homologue.[42] Removal of the autoinhibitory domain from HR1a is, however, not sufficient for full activation of the kinase,[20] and therefore, it is possible that HR1b interactions are also required, pointing to an important role for the Rac1−HR1b interaction in controlling levels of PRK1 activation.

In summary, we have confirmed contact II as the true solution binding interface between RhoA and PRK1 HR1a. We have also shown that the HR1a and HR1b domains from PRK1 have different thermal stabilities. The helical content of the HR1ab didomain, as determined by CD, was greater than that predicted by combining the known helical contents of the two isolated domains; thus, expressing the two domains in tandem alters the secondary structure of the domains in an, as yet, undetermined manner. Li et al.[36] found that residues 7−155 of PRK1 were not completely folded at 4 °C, and taken together with our data, this suggests that the adjacent HR1 domains in the PRKs may influence one another structurally and may be more than just isolated protein-binding modules. Most of the HR1a domains, e.g., from PRKs, rhotekins, and rhophilins, are located at the N-termini of their respective proteins. It would be interesting to determine whether this conserved location is important for their biological function. The thermal stability of the HR1a domain is significantly lower than that of the HR1b domain, and it is possible that this implies that this larger degree of conformational flexibility allows HR1a to bind tightly to both RhoA and Rac1.

■ ASSOCIATED CONTENT

Supporting Information. Derivation of eq 3. This material is available free of charge via the Internet at http://pubs.acs.org.

AUTHOR INFORMATION

Corresponding Author

*Telephone: +44-1223-764824. Fax: +44-1223-766002. E-mail: do@bioc.cam.ac.uk.

Funding Sources

This research was supported by a BBSRC Studentship to C.L.H., CR-UK Project Grant C11309/A5148 (to D.O. and H.R.M.), and MRC Project Grant G0700057 (to D.O. and H.R.M.).

ACKNOWLEDGMENT

We thank Dr. Joseph Maman (Department of Biochemistry, University of Cambridge) for help with initial acquisition of CD data on the AVIV 410 instrument. We also thank Dr. Laura Itzhaki (Hutchison/MRC Research Centre, Cambridge, U.K.) for allowing us access to the Applied Photophysics Chirascan spectrometer and Dr. Pam Rowling for help with the experimental setup.

ABBREVIATIONS

RBD, Rho protein binding domain; PRK, protein kinase C-related kinase; HR1, homology region 1; IPTG, isopropyl β-D-thiogalactopyranoside; GST, glutathione *S*-transferase; GTP, guanosine 5′-triphosphate; GDP, guanosine 5′-diphosphate; DTT, dithiothreitol; SPA, scintillation proximity assays; CD, circular dichroism.

REFERENCES

(1) Ridley, A. J., Allen, W. E., Peppelenbosch, M., and Jones, G. E. (1999) Rho family proteins and cell migration. *Biochem. Soc. Symp.*, 111–123.

(2) Govek, E. E., Newey, S. E., and Van Aelst, L. (2005) The role of the Rho GTPases in neuronal development. *Genes Dev. 19*, 1–49.

(3) Salminen, A., Suuronen, T., and Kaarniranta, K. (2008) ROCK, PAK, and Toll of synapses in Alzheimer's disease. *Biochem. Biophys. Res. Commun. 371*, 587–590.

(4) Mueller, B. K., Mack, H., and Teusch, N. (2005) Rho kinase, a promising drug target for neurological disorders. *Nat. Rev. Drug Discovery 4*, 387–398.

(5) Budzyn, K., Marley, P. D., and Sobey, C. G. (2006) Targeting Rho and Rho-kinase in the treatment of cardiovascular disease. *Trends Pharmacol. Sci. 27*, 97–104.

(6) Vega, F. M., and Ridley, A. J. (2008) Rho GTPases in cancer cell biology. *FEBS Lett. 582*, 2093–2101.

(7) Fujisawa, K., Madaule, P., Ishizaki, T., Watanabe, G., Bito, H., Saito, Y., Hall, A., and Narumiya, S. (1998) Different regions of Rho determine Rho-selective binding of different classes of Rho target molecules. *J. Biol. Chem. 273*, 18943–18949.

(8) Palmer, R. H., Ridden, J., and Parker, P. J. (1995) Cloning and Expression Patterns of 2 Members of a Novel Protein-Kinase-C-Related Kinase Family. *Eur. J. Biochem. 227*, 344–351.

(9) Watanabe, G., Saito, Y., Madaule, P., Ishizaki, T., Fujisawa, K., Morii, N., Mukai, H., Ono, Y., Kakizuka, A., and Narumiya, S. (1996) Protein kinase N (PKN) and PKN-related protein rhophilin as targets of small GTPase Rho. *Science 271*, 645–648.

(10) Mukai, H. (2003) The structure and function of PKN, a protein kinase having a catalytic domain homologous to that of PKC. *J. Biochem. 133*, 17–27.

(11) Mukai, H., Toshimori, M., Shibata, H., Kitagawa, M., Shimakawa, M., Miyahara, M., Sunakawa, H., and Ono, Y. (1996) PKN associates and phosphorylates the head-rod domain of neurofilament protein. *J. Biol. Chem. 271*, 9816–9822.

(12) Matsuzawa, K., Kosako, H., Inagaki, N., Shibata, H., Mukai, H., Ono, Y., Amano, M., Kaibuchi, K., Matsuura, Y., Azuma, I., and Inagaki, M. (1997) Domain-specific phosphorylation of vimentin and glial fibrillary acidic protein by PKN. *Biochem. Biophys. Res. Commun. 234*, 621–625.

(13) Kawamata, T., Taniguchi, T., Mukai, H., Kitagawa, M., Hashimoto, T., Maeda, K., Ono, Y., and Tanaka, C. (1998) A protein kinase, PKN, accumulates in Alzheimer neurofibrillary tangles and associated endoplasmic reticulum-derived vesicles and phosphorylates tau protein. *J. Neurosci. 18*, 7402–7410.

(14) Metzger, E., Muller, J. M., Ferrari, S., Buettner, R., and Schule, R. (2003) A novel inducible transactivation domain in the androgen receptor: implications for PRK in prostate cancer. *EMBO J. 22*, 270–280.

(15) Gao, Q. S., Kumar, A., Srinivasan, S., Singh, L., Mukai, H., Ono, Y., Wazer, D. E., and Band, V. (2000) PKN binds and phosphorylates human papillomavirus E6 oncoprotein. *J. Biol. Chem. 275*, 14824–14830.

(16) Quilliam, L. A., Lambert, Q. T., MickelsonYoung, L. A., Westwick, J. K., Sparks, A. B., Kay, B. K., Jenkins, N. A., Gilbert, D. J., Copeland, N. G., and Der, C. J. (1996) Isolation of a NCK-associated kinase, PRK2, an SH3-binding protein and potential effector of Rho protein signaling. *J. Biol. Chem. 271*, 28772–28776.

(17) Vincent, S., and Settleman, J. (1997) The PRK2 kinase is a potential effector target of both Rho and Rac GTPases and regulates actin cytoskeletal organization. *Mol. Cell. Biol. 17*, 2247–2256.

(18) Takahashi, M., Mukai, H., Toshimori, M., Mlyamoto, M., and Ono, Y. (1998) Proteolytic activation of PKN by caspase-3 or related protease during apoptosis. *Proc. Natl. Acad. Sci. U.S.A. 95*, 11566–11571.

(19) Dong, L. Q., Landa, L. R., Wick, M. J., Zhu, L., Mukai, H., Ono, Y., and Liu, F. (2000) Phosphorylation of protein kinase N by phosphoinositide-dependent protein kinase-1 mediates insulin signals to the actin cytoskeleton. *Proc. Natl. Acad. Sci. U.S.A. 97*, 5089–5094.

(20) Yoshinaga, C., Mukai, H., Toshimori, M., Miyamoto, M., and Ono, Y. (1999) Mutational analysis of the regulatory mechanism of PKN: The regulatory region of PKN contains an arachidonic acid-sensitive autoinhibitory domain. *J. Biochem. 126*, 475–484.

(21) Flynn, P., Mellor, H., Palmer, R., Panayotou, G., and Parker, P. J. (1998) Multiple interactions of PRK1 with RhoA: Functional assignment of the HR1 repeat motif. *J. Biol. Chem. 273*, 2698–2705.

(22) Owen, D., Lowe, P. N., Nietlispach, D., Brosnan, C. E., Chirgadze, D. Y., Parker, P. J., Blundell, T. L., and Mott, H. R. (2003) Molecular dissection of the interaction between the small G proteins Rac1 and RhoA and protein kinase C-related kinase 1 (PRK1). *J. Biol. Chem. 278*, 50578–50587.

(23) Blumenstein, L., and Ahmadian, M. R. (2004) Models of the cooperative mechanism for Rho effector recognition: Implications for RhoA-mediated effector activation. *J. Biol. Chem. 279*, 53419–53426.

(24) Maesaki, R., Ihara, K., Shimizu, T., Kuroda, S., Kaibuchi, K., and Hakoshima, T. (1999) The structural basis of Rho effector recognition revealed by the crystal structure of human RhoA complexed with the effector domain of PKN/PRK1. *Mol. Cell 4*, 793–803.

(25) Modha, R., Campbell, L. J., Nietlispach, D., Buhecha, H. R., Owen, D., and Mott, H. R. (2008) The Rac1 Polybasic Region Is Required for Interaction with Its Effector PRK1. *J. Biol. Chem. 283*, 1492–1500.

(26) Strugnell, S. A., Wiefling, B. A., and DeLuca, H. F. (1997) A modified pGEX vector with a C-terminal histidine tag: Recombinant double-tagged protein obtained in greater yield and purity. *Anal. Biochem. 254*, 147–149.

(27) Long, A. C., Orr, D. C., Cameron, J. M., Dunn, B. M., and Kay, J. (1989) A Consensus Sequence for Substrate Hydrolysis by Rhinovirus 3c Proteinase. *FEBS Lett. 258*, 75–78.

(28) Mach, H., Middaugh, C. R., and Lewis, R. V. (1992) Statistical Determination of the Average Values of the Extinction Coefficients of Tryptophan and Tyrosine in Native Proteins. *Anal. Biochem. 200*, 74–80.

(29) Fenwick, R. B., Prasannan, S., Campbell, L. J., Nietlispach, D., Evetts, K. A., Camonis, J., Mott, H. R., and Owen, D. (2009) Solution Structure and Dynamics of the Small GTPase RalB in Its Active Conformation: Significance for Effector Protein Binding. *Biochemistry 48*, 2192–2206.

(30) Graham, D. L., Eccleston, J. F., and Lowe, P. N. (1999) The conserved arginine in Rho-GTPase-activating protein is essential for efficient catalysis but not for complex formation with rho CDP and aluminum fluoride. *Biochemistry 38*, 985–991.

(31) Whitmore, L., and Wallace, B. A. (2004) DICHROWEB, an online server for protein secondary structure analyses from circular dichroism spectroscopic data. *Nucleic Acids Res. 32*, W668–W673.

(32) Whitmore, L., and Wallace, B. A. (2008) Protein secondary structure analyses from circular dichroism spectroscopy: Methods and reference databases. *Biopolymers 89*, 392–400.

(33) Compton, L. A., and Johnson, W. C. (1986) Analysis of Protein Circular-Dichroism Spectra for Secondary Structure Using a Simple Matrix Multiplication. *Anal. Biochem. 155*, 155–167.

(34) Sreerama, N., and Woody, R. W. (2000) Analysis of protein CD spectra: Comparison of CONTIN, SELCON3, and CDSSTR methods in CDPro software. *Biophys. J. 78*, 334A–334A.

(35) Fenwick, R. B., Campbell, L. J., Rajasekar, K., Prasannan, S., Nietlispach, D., Camonis, J., Owen, D., and Mott, H. R. (2010) The RaIB-RLIP76 Complex Reveals a Novel Mode of RaI-Effector Interaction. *Structure 18*, 985–995.

(36) Li, Y., Kaur, H., and Oakley, M. G. (2008) Probing the recognition properties of the antiparallel coiled coil motif from PKN by protein grafting. *Biochemistry 47*, 13564–13572.

(37) Linding, R., Russell, R. B., Neduva, V., and Gibson, T. J. (2003) GlobPlot: Exploring protein sequences for globularity and disorder. *Nucleic Acids Res. 31*, 3701–3708.

(38) Rost, B., Yachdav, G., and Liu, J. F. (2004) The PredictProtein server. *Nucleic Acids Res. 32*, W321–W326.

(39) Moreira, I. S., Fernandes, P. A., and Ramos, M. J. (2007) Hot spots: A review of the protein−protein interface determinant amino-acid residues. *Proteins 68*, 803–812.

(40) Elliot-Smith, A. E., Mott, H. R., Lowe, P. N., Laue, E. D., and Owen, D. (2005) Specificity Determinants on Cdc42 for Binding Its Effector Protein ACK. *Biochemistry 44*, 12373–12383.

(41) Kitagawa, M., Shibata, H., Toshimori, M., Mukai, H., and Ono, Y. (1996) The role of the unique motifs in the amino-terminal region of PKN on its enzymatic activity. *Biochem. Biophys. Res. Commun. 220*, 963–968.

(42) Lu, Y., and Settleman, J. (1999) The *Drosophila* Pkn protein kinase is a Rho Rac effector target required for dorsal closure during embryogenesis. *Genes Dev. 13*, 1168–1180.